

# High-capacity adenoviral vector-mediated expression of an LDLR/transferrin chimeric protein in muscle reduces atherosclerosis in *Ldlr*<sup>-/-</sup> mice

Maria Vitale,<sup>1,2,11</sup> Filippo Scialò,<sup>1,3,11</sup> Ludovica Coluccino,<sup>1,3</sup> Anna D'Agostino,<sup>4</sup> Lorella Tripodi,<sup>1,3</sup> Raffaella Pagliaro,<sup>5,6</sup> Andrea Bianco,<sup>5,6</sup> Giuseppe Castaldo,<sup>1,3</sup> Vincenzo Cerullo,<sup>1,3,7,8,9,10</sup> and Lucio Pastore<sup>1,3</sup>

<sup>1</sup>CEINGE-Biotecnologie Avanzate Franco Salvatore, 80145 Naples, Italy; <sup>2</sup>Kimera s.r.l., Via Gaetano Filangieri 48, 80121 Naples, Italy; <sup>3</sup>Dipartimento di Medicina Molecolare e Biotecnologie Mediche, Università degli Studi di Napoli Federico II, 80131 Naples, Italy; <sup>4</sup>IRCCS SYNLAB SDN Institute, Via Galileo Ferraris 144, 80143 Naples, Italy; <sup>5</sup>Dipartimento di Scienze Mediche Traslazionali, Università della Campania "L. Vanvitelli", 80131 Naples, Italy; <sup>6</sup>U.O.C. Clinica Pneumologica L. Vanvitelli, A.O. dei Colli, Monaldi Hospital, 80131 Naples, Italy; <sup>7</sup>Drug Research Program (DRP), ImmunoViroTherapy Lab (IVT), Division of Pharmaceutical Biosciences, Faculty of Pharmacy, University of Helsinki, 00014 Helsinki, Finland; <sup>8</sup>Helsinki Institute of Life Science (HiLIFE), University of Helsinki, 00014 Helsinki, Finland; <sup>9</sup>Translational Immunology Program (TRIMM), Faculty of Medicine, University of Helsinki, 00014 Helsinki, Finland; <sup>10</sup>Digital Precision Cancer Medicine Flagship (iCAN), University of Helsinki, 00014 Helsinki, Finland

**Familial hypercholesterolemia (FH) is a genetic disorder caused by mutations in the low-density lipoprotein (LDL) receptor, leading to impaired uptake of LDL and its accumulation in arterial walls and other tissues. This accumulation results in cardiovascular disease and early mortality. Treatments, including statins, ezetimibe, PCSK9 inhibitors, and bempedoic acid, are often insufficient in homozygous FH patients, particularly those with null mutations in the LDL receptor (LDLR). To address this unmet need, we have developed two helper-dependent adenoviral (HD-Ad) vectors for the expression of the murine and human versions of a protein composed of the extracellular portion of the LDLR fused to transferrin. In both cassettes, expression is driven by the murine creatine kinase promoter to obtain high levels of expression restricted to muscle cells, to mitigate host response to the fusion protein. Both human and murine proteins restored LDL uptake in *Ldlr*-deficient cells, correcting the phenotype *in vitro*. A single intramuscular administration of the HD-Ad vector induced the expression of the murine fusion protein, leading to a 12-month improvement in the lipid profile, with a reduction in aortic atherosclerosis in *Ldlr*-deficient mice. Furthermore, we observed no major systemic toxicity, indicating that the present strategy may represent more effective therapy for FH patients.**

## INTRODUCTION

Familial hypercholesterolemia (FH) is an autosomal genetic condition characterized by levels of low-density lipoprotein cholesterol (LDL-C) exceeding 190 mg/dL, with consequent development of premature atherosclerotic lesions.<sup>1,2</sup> The most common causative mutations are in the LDL receptor (LDLR) gene accounting for 60%–80% of cases.<sup>3,4</sup> In addition to LDLR mutations, variants in

the apolipoprotein B (APOB) gene and gain-of-function mutations in the proprotein convertase subtilisin/kexin type 9 (PCSK9) gene can cause FH. The clinical manifestations of FH are heterogeneous; while some patients exhibit physical signs such as tendon xanthomas or premature corneal arcus, others remain asymptomatic until they experience a cardiovascular event.<sup>2,5</sup>

LDLR is a cell surface glycoprotein that plays a crucial role in the receptor-mediated endocytosis of LDL. LDLR and transferrin receptor (TFRC) have similar uptake mechanisms: in both pathways, the receptor-ligand complexes are clustered in clathrin-coated pits on the plasma membrane, leading to the formation and internalization of vesicles. Once inside the cells, the acidic environment of the endosome triggers the dissociation of the receptor-ligand complexes. The receptors dissociated from the complexes are recycled back to the plasma membrane, ensuring the capture of more ligands.<sup>6–9</sup>

Mutations in the LDLR gene that can lead to complete protein absence and loss of function are known as class 1 mutations, whereas class 2–5 mutations affect LDL uptake or receptor degradation, ultimately increasing LDL-C levels.<sup>2,10</sup> The management of homozygote FH patients requires reduction of LDL-C plasma levels with a multifaceted approach that combines lifestyle modifications and several treatments with drugs such as statins, ezetimibe, PCSK9 inhibitors,<sup>11</sup> bile acid sequestrants, niacin, fibrates, bempedoic acid, and LDL apheresis.<sup>12–15</sup> Although current treatments often involve

Received 29 April 2025; accepted 4 February 2026;  
<https://doi.org/10.1016/j.ymthe.2026.02.014>

<sup>11</sup>These authors contributed equally

**Correspondence:** Lucio Pastore, CEINGE-Biotecnologie Avanzate Franco Salvatore, 80145 Naples, Italy.

**E-mail:** [lucio.pastore@unina.it](mailto:lucio.pastore@unina.it)

multiple drugs to lower plasma LDL-C levels, new therapeutic approaches are needed. These novel strategies should not only enhance lipid-lowering efficacy but also reduce side effects and possibly eliminate the need for frequent administration.<sup>13</sup>

Gene replacement therapy approaches are usually aimed at inducing long-term expression of therapeutic transgenes<sup>16-19</sup> to overcome the need of lifelong treatments for patients to provide a long-lasting cure. These strategies are particularly relevant for homozygous patients, who often fail to achieve desirable LDL-C levels. Gene therapy strategies typically transduce a functional version of the altered gene into target cells using either viral<sup>20-22</sup> or non-viral approaches.<sup>23</sup> Most gene transfer strategies developed for FH therapy have focused on liver-directed transduction of a functional copy of the LDLR<sup>18,24-26</sup> or, alternatively, the very-low-density lipoprotein receptor (VLDLR)<sup>19</sup>; in fact, in *Ldlr*-deficient mice, helper-dependent adenoviral (HD-Ad) vector-mediated overexpression of *Vldlr* is associated with long-lasting and stable amelioration of lipid profile and reduction of aortic atherosclerotic plaque deposition.<sup>19</sup> Furthermore, HD-Ad-mediated overexpression of human APOA1 (hAPOA1) resulted in increased high-density lipoprotein -cholesterol (HDL-C) levels, efficiently reducing aortic atherosclerotic plaques in both *Apoe*- and *Ldlr*-deficient mice.<sup>17,27</sup>

In recent years, we have developed an alternative therapeutic strategy based on the expression of a secreted fusion protein. This protein is composed of the extracellular portion of the human LDLR, which is able to bind Ldl and is linked to rabbit transferrin (Tf). Rabbit Tf binds the transferrin receptor (Tfrc), resulting in internalization and uptake of Ldl particles.<sup>8,19,28</sup> We have previously developed a HD-Ad vector for the expression of the LDLR/Tf fusion protein under the control of the transthyretin promoter. After intravenous (IV) administration in *Ldlr*-deficient mice, we observed LDLR/Tf expression and secretion in the bloodstream, leading to long-lasting amelioration of lipid profiles and a consequent reduction in aortic atherosclerosis, surpassing the short-term results previously achieved with a non-viral approach.<sup>28</sup>

To further improve both efficacy and safety of this strategy, in the present study, we developed cassettes for the expression of either the murine (mLdlr/mTf) or the human (hLDLR/hTF) version of fusion protein, under the control of the muscle-specific murine creatine kinase (mCK) promoter. We inserted these cassettes in HD-Ad vectors to evaluate their efficacy *in vitro* and *in vivo*. We used these vectors to infect the differentiated C2C12 myoblastoid cells to evaluate fusion protein expression. In addition, treatment with supernatants of infected C2C12 cells, containing the fusion proteins, was able to restore LDL uptake in the CHOldIA7, an *Ldlr*-deficient cell line. We then intramuscularly (IM) administered the HD-Ad vector expressing mLdlr/mTf, observing a long-lasting amelioration of the lipid profile with a consequent reduction in aortic atherosclerosis in the absence of significant short- and long-term toxicity.

## RESULTS

### HD-Ad vector-mediated expression of fusion protein in C2C12 cells resulted in expression and secretion of functional proteins

mLdlr/mTf and hLDLR/hTF sequences were designed *in silico* by fusing the N-terminal coding sequence of either mLdlr or hLDLR with mTf or hTF. Codon usage was optimized for species-specific expression; in addition, to enhance mRNA stability and increase protein expression, we incorporated the woodchuck hepatitis virus post-transcriptional regulatory element (WPRE) and the antisense SV40 polyadenylation signal. Both mLdlr/mTf and hLDLR/hTF cDNAs were under the control of the muscle-specific mCK promoter to obtain efficient protein expression after IM administration (Figure 1A). To assess the ability of HD-Ad-mLdlr/mTf and HD-Ad-hLDLR/hTF to induce expression and secretion of the chimeric murine and human fusion protein, respectively, we infected C2C12, a murine cell line that can be differentiated into myoblasts, with 100 or 200 multiplicities of infection (MOIs, viral particles [vp] per cell) of vectors. We collected the supernatant of infected and differentiated C2C12 cells and determined the expression and secretion of mLdlr/mTf and hLDLR/hTF proteins by western blot analysis (Figure 1B). To evaluate whether both mLdlr/mTf and hLDLR/hTF proteins were able to bind and restore LDL uptake, we infected C2C12 cells with 100 MOIs of HD-Ad-mLdlr/mTf, HD-Ad-hLDLR/hTF, or an empty vector as negative control, using a lipoprotein-free medium. Cell supernatants were then harvested, purified to remove cell debris, and used to treat, in a lipoprotein-free medium, CHOldIA7 cells that lack *Ldlr* function. We then added fluorescently labeled LDL and observed their uptake in CHOldIA7 cells treated with supernatants of C2C12 cells infected with either HD-Ad-mLdlr/mTf or HD-Ad-hLDLR/hTF; CHOldIA7 cells treated with supernatants of C2C12 cells infected with the control vector did not result in fluorescently labeled LDL uptake (Figure 1C).

### IM administration of a HD-Ad vector expressing *Ldlr*/Tf does not induce significant systemic toxicity in *Ldlr*-deficient mice

After evaluating the ability of HD-Ad-mLdlr/mTf to infect *in vitro* differentiated myoblasts and induce expression and secretion of a functional mLdlr/mTf protein, we decided to evaluate major systemic toxicity of IM administration of this vector. We administered  $1 \times 10^{13}$  vp/kg HD-Ad-mLdlr/mTf in the quadriceps of 5 male *Ldlr*-deficient mice (Figure 2A); a control group was treated with PBS. We collected blood from both groups 6 h after administration and determined interleukin-6 (IL-6) and IL-12 levels; these cytokines are associated with the activation of the innate immune response. We also determined D-dimer levels to evaluate possible intravascular coagulation. We chose to evaluate these markers 6 h after administration because in previous studies, after IV viral administration, peaks of these cytokines were observed at this time point, followed by a rapid return to baseline levels after 24 h. We did not observe significant differences in serum IL-12 and IL-6 levels between treated and control mice (Figures 2B and 2C); in fact, average serum levels of IL-12 were  $1,685.39 \pm 92.97$  pg/mL in PBS-treated mice and

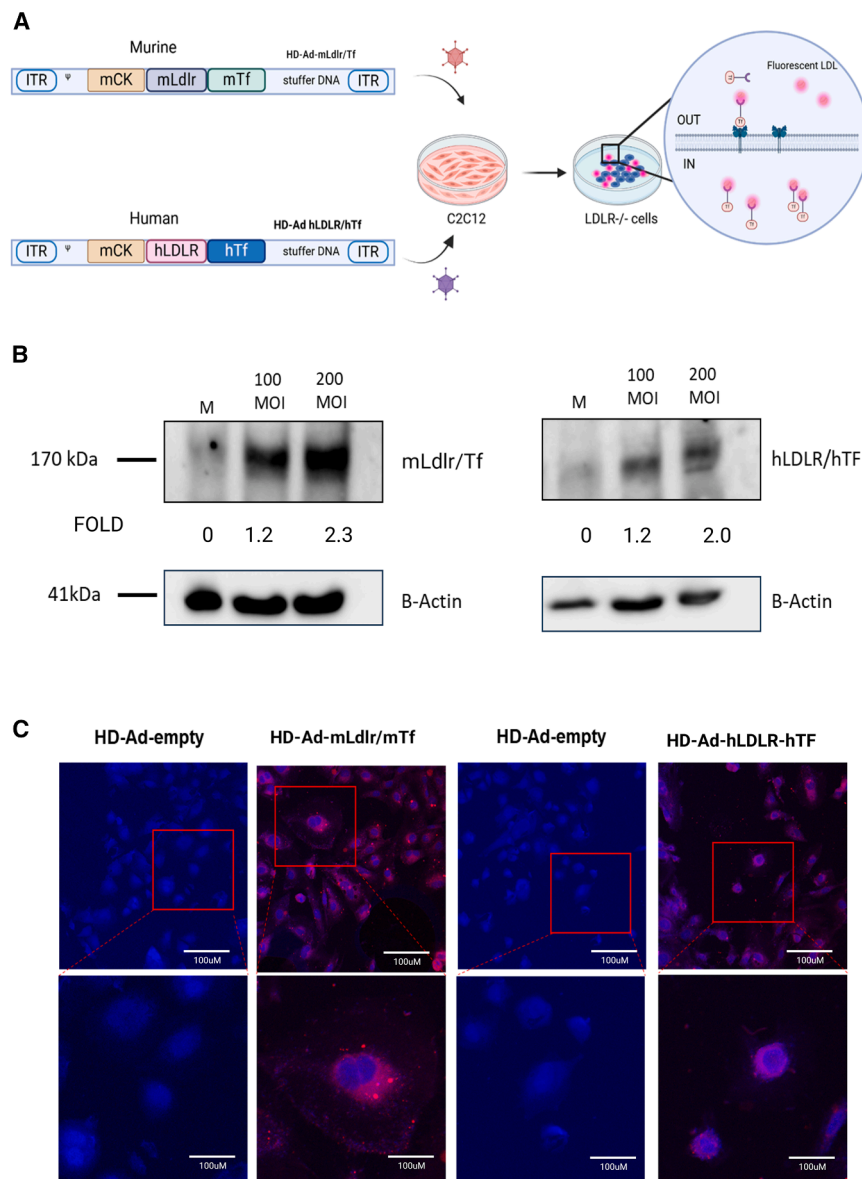


**Figure 1. Myoblast cell line infection with HD-Ad vectors expressing either murine or human fusion protein results in the secretion of functional proteins**

(A) A schematic representation of the HD-Ad vectors containing the cassettes for the muscle-specific expression of either murine (mLdlr/mTf) or human (hLDLR/hTF) chimeric proteins; these vectors induce fusion protein expression in a murine myoblast cell line, and the proteins present in the supernatant can restore LDL uptake in an *Ldlr*-deficient cell line. (B) Western blot analysis of C2C12 differentiated myoblast lysate infected with 100 and 200 MOIs of either HD-Ad-mLdlr/mTf or HD-Ad-hLDLR/hTF confirms the expression of the 170-kDa chimeric protein. M indicates the lysates from mock-treated cells. Western blots were quantified by ImageJ (NIH), and band intensities (reported below) were expressed as ratio normalized on the loading control signals. (C) CHOIdIA7 cells were treated with supernatant from C2C12 cells infected with 100 MOIs of either HD-Ad-mLdlr/mTf or HD-Ad-hLDLR/hTF. Dil-LDL<sup>+</sup> endocytic vesicles were observed in cells treated with the chimeric protein-containing supernatant. Dil-LDL incorporation was analyzed by confocal microscopy.

**IM administration of a HD-Ad vector expressing mLdlr/mTf ameliorates lipid profile and reduces aortic atherosclerosis in *Ldlr*-deficient mice**

After *in vitro* assessment of the ability of the fusion mLdlr/mTf protein to restore LDL uptake and observation of the absence of major systemic toxicity, we evaluated the efficacy of our approach in improving lipid profiles and reducing aortic atherosclerosis. We then administered  $1 \times 10^{13}$  vp/kg of the HD-Ad-mLdlr/mTf vector in the right quadriceps of 5 male *Ldlr*-deficient mice, and a control group of mice was treated with PBS. To strengthen the translational relevance of our findings, we included human-equivalent dose estimates

based on allometric scaling; the dose of  $1 \times 10^{13}$  vp/kg in mice corresponds to approximately  $8 \times 10^{11}$  vp/kg in humans, a level consistent with the tolerability observed in large-animal studies.

We evaluated lipid profiles of treated and control mice for 12 weeks and then evaluated aortic atherosclerosis. We collected blood samples from both groups at different time points and assessed the presence of the fusion protein in plasma from mice treated with HD-Ad-mLdlr/mTf using western blot analysis. A polyclonal antibody against *Ldlr* detected the protein, revealing a band around 170 kDa in treated mice that was absent in the PBS-treated group (Figure 3A). Total cholesterol (TC), LDL-C, high-density lipoprotein cholesterol (HDL-C), and triglycerides (TG) levels were evaluated before treatment (time 0) and, subsequently, 1, 2, 6, 8, and 12 weeks

1,756.81 ± 73.12 pg/mL in treated mice, whereas IL-6 serum levels were 375.801 ± 9.03 and 355.467 ± 17.06 pg/mL, respectively. Similarly, we did not observe significant differences in D-dimer levels between treated and control mice (83.615 ± 3.17 and 79.811 ± 3.14 pg/mL; Figure 2D). To evaluate liver toxicity, we evaluated serum alanine aminotransferase (ALT) and aspartate aminotransferase (AST) levels 72 h after vector administration. We did not observe significant differences in ALT and AST levels between treated and control groups (Figures 2E and 2F). Furthermore, to evaluate long-term hepatotoxicity, transaminases serum levels were determined 3, 14, 56, and 85 days after treatment (Figures 2G and 2H). Transaminase serum levels were in the normal range at each time point analyzed, and no significant differences were observed between control and treated groups (Table 1).

based on allometric scaling; the dose of  $1 \times 10^{13}$  vp/kg in mice corresponds to approximately  $8 \times 10^{11}$  vp/kg in humans, a level consistent with the tolerability observed in large-animal studies.

We evaluated lipid profiles of treated and control mice for 12 weeks and then evaluated aortic atherosclerosis. We collected blood samples from both groups at different time points and assessed the presence of the fusion protein in plasma from mice treated with HD-Ad-mLdlr/mTf using western blot analysis. A polyclonal antibody against *Ldlr* detected the protein, revealing a band around 170 kDa in treated mice that was absent in the PBS-treated group (Figure 3A). Total cholesterol (TC), LDL-C, high-density lipoprotein cholesterol (HDL-C), and triglycerides (TG) levels were evaluated before treatment (time 0) and, subsequently, 1, 2, 6, 8, and 12 weeks

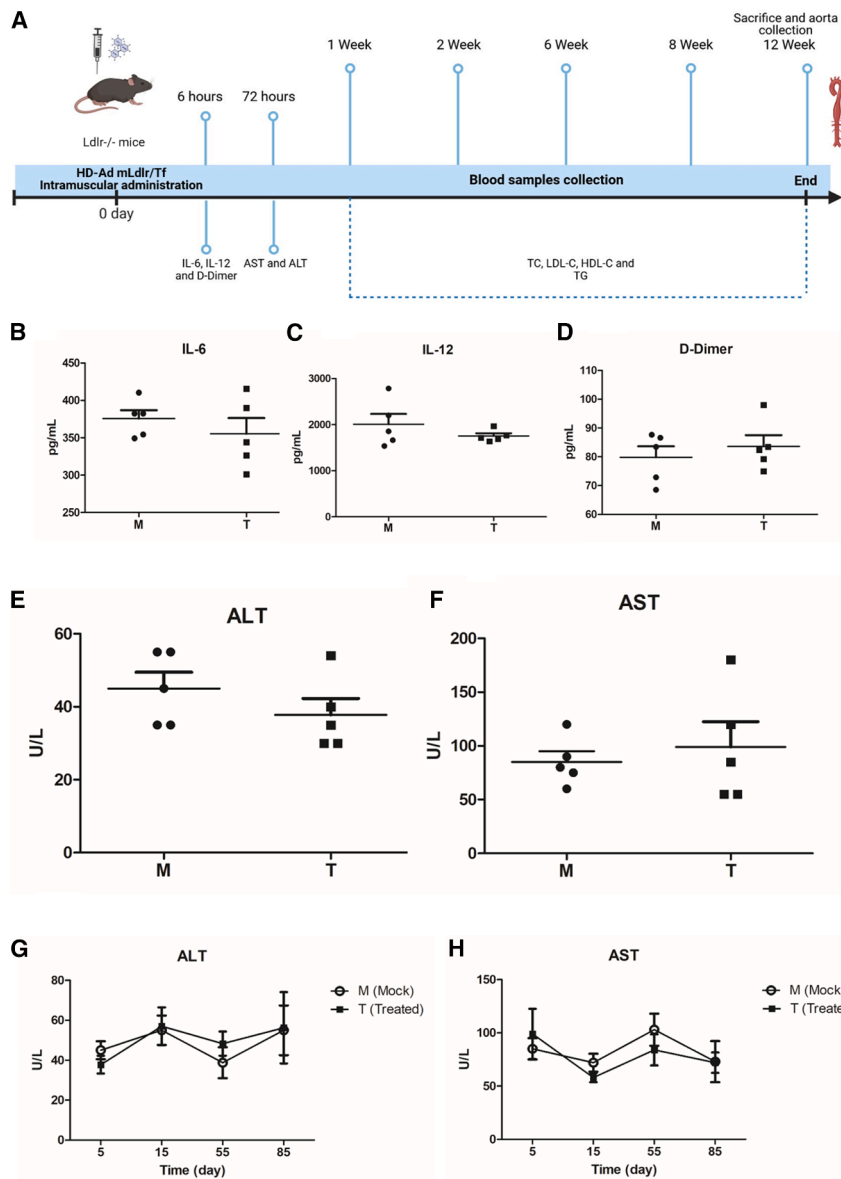


**Figure 2. Intramuscular administration of HD-Ad-mLdlr/mTf in *Ldlr*-deficient mice does not induce an innate response and does not cause liver damage**

(A) Time points of the experiment: two groups of *Ldlr*-deficient mice ( $n = 5$ ) were treated with intramuscular (IM) administration of either  $1.0 \times 10^{13}$  vp/kg of HD-Ad-mLdlr/mTf or PBS. Six hours after administration, we collected blood samples from each mouse to determine IL-6, IL-12, and D-dimer levels. We collected additional blood samples 72 h after administration to determine AST and ALT levels. Lipid profiles, including total cholesterol (TC), LDL-C, HDL-C, and triglycerides (TG) were determined in mice from both groups at 1, 2, 6, 8, and 12 weeks after administration. (B) HD-Ad-mLdlr/mTf administration does not cause a significant increase in serum IL-6 levels compared with the PBS-treated group. (C) HD-Ad-mLdlr/mTf administration does not cause a significant increase in serum IL-12 levels compared with the PBS-treated group. (D) HD-Ad-mLdlr/mTf administration does not cause a significant increase in D-dimer levels compared with the PBS-treated group. Data shown as mean  $\pm$  SEM of duplicate technical replicates and expressed in pg/mL. (E and F) Plasma levels of ALT and AST were measured 3 days after treatment administration to assess potential liver toxicity. Plasma samples were collected from both the saline control group (M) and the virus-treated group (T) under identical conditions. Results were expressed as units per liter (U/L) and reported as mean  $\pm$  SEM. (G and H) ALT and AST levels were assessed at 5, 15, 55, and 85 days following IM injection of the viral vector. Results were expressed as U/L and presented as mean  $\pm$  SEM. M represents the PBS-treated control group, while T indicates the group treated with IM HD-Ad.

after treatment. Baseline TG were  $165.2 \pm 21.4$  and  $158.4 \pm 11.5$  mg/dL for the control and the treated group, respectively. We observed a significant reduction of TG levels 1 week after treatment in treated mice compared with the control group ( $93.3 \pm 11.6$  and  $185 \pm 17.2$ , respectively; **Figure 3B**). Decreased TG levels were maintained in treated mice for the entire duration of the experiment. LDL-C levels were similar between control and treated animals at time 0 ( $167.7 \pm 36.9$  and  $156.7 \pm 41.1$  mg/dL, respectively). One week after treatment, LDL-C levels in the treated group significantly decreased to  $60.48 \pm 6.5$  mg/dL. LDL-C reduction was maintained for the entire duration of the experiment (**Figure 3C**). Basal HDL-C levels were also similar between control and treated groups ( $106.8 \pm 13.7$  and  $118.8 \pm 18.8$  mg/dL, respectively); HDL-C also decreased to  $74.8 \pm 9.9$  mg/dL 1 week after treatment (**Figure 3D**); and reduction of

1 week after treatments to  $154 \pm 8.8$  mg/dL in treated mice while remaining almost stable in the control group ( $398.8 \pm 48.8$  mg/dL; **Figure 3E**). We assessed the impact of IM expression of the chimeric *Ldlr*/Tf protein on the progression of aortic atherosclerosis. Twelve weeks post-treatment, we sacrificed the experimental mice, dissected the aortas from the heart to the iliac branching, and carefully removed external fat and residual tissue. We then performed oil red O (ORO) staining and analyzed aortic atherosclerotic areas using an en face method. Untreated mice exhibited more pronounced atherosclerotic lesions compared with treated mice (**Figure 3F**). The lesion areas were significantly smaller in the treated group, covering only 4.2% of the aortic surface, compared with 17.4% in the control group (**Figure 3G**). Finally, to confirm our data, we evaluated fusion protein transcript levels in skeletal muscle and liver.

**Table 1. Serum transaminase levels after IM administration of HD-Ad mLdlr/mTf in Ldlr-deficient mice**

Day	Treated		Mock	
	AST, U/L	ALT, U/L	AST, U/L	ALT, U/L
5	99 ± 23.5	37.8 ± 4.4	85 ± 10	45 ± 4.4
15	58 ± 4.3	57 ± 9.4	72 ± 8.4	74 ± 19.8
55	84 ± 14.6	94 ± 31.4	103 ± 15.0	69 ± 30.8
85	72 ± 9.5	73 ± 21.7	73 ± 19.2	81 ± 27.7
Normal range	72–288	24–140	–	–

Data are reported as mean ± SEM of five mice per group ( $n = 5$ ). ALT, alanine aminotransferase; AST, aspartate aminotransferase; HD-Ad, helper-dependent adenoviral; IM, intramuscular; Ldlr, low-density lipoprotein receptor; mLdlr, murine Ldlr; mTf, murine transferrin.

This analysis revealed that the fusion protein was expressed in the muscle of treated mice (Figure 3H), where a significant increase was observed compared with untreated controls ( $p = 0.0031$ ). In contrast, no significant difference in transgene expression was detected in the liver between untreated (mock) and treated animals.

## DISCUSSION

Over the years, several gene transfer strategies have been developed for the treatment of FH.<sup>17,30–32</sup> Early approaches have relied on *ex vivo* gene therapy, with unsuccessful results.<sup>19</sup> HD-Ad vectors lack all viral genes that result in reduced toxicity, maintaining the ability of efficiently transducing cells to lead to long-term transgene expression, compared with first-generation adenoviral (FG-Ad) vectors.<sup>33</sup> Several animal models of monogenic disorders have been corrected with gene replacement strategies using HD-Ad vector administration in the absence of chronic toxicity<sup>34,35</sup>; a paradigmatic example is the correction of hypercholesterolemia in apoe-deficient mice<sup>17,34</sup> or in Ldlr-deficient mice.<sup>28</sup> Greig et al. demonstrated phenotype correction in FH mouse and rhesus monkey models using an adeno-associated virus serotype 8 (AAV8)-based vector.<sup>36,37</sup> However, the subsequent clinical trial has been halted, and this strategy has not reached a full clinical application. A recent strategy based on the inactivation of the PCSK9 gene in patients with an *in vivo* base editing approach has been successful in FH patients<sup>11</sup>; however, PCSK9 inactivation-based strategies rely on the presence of residual LDLR activity that is not always present in homozygous FH patients.

IV administration of viral vectors has been associated with relevant toxicity, even with the safer AAV vectors.<sup>38,39</sup> FG-Ad and second-generation Ad vectors induce a relevant very early host response that has proven to be potentially lethal<sup>40,41</sup>; in addition, accumulation of viral proteins in transduced cells induces cell death and reduced efficacy.<sup>42</sup> Despite the absence of chronic toxicity after IV administration of HD-Ad vectors, acute host response was observed shortly after treatment in animal models<sup>32</sup>; this reaction is not due to the expression of viral proteins but is caused by viral capsid proteins that induce inflammatory response.<sup>33</sup> The severity of acute toxicity is dose dependent and is not observed at low viral doses; unfortunately, at these doses, hepatic transduction is negligible.<sup>43,44</sup> Acute toxicity

after Ad administration results in an increase in the serum of pro-inflammatory cytokines (IL-12, IL-6, and tumor necrosis factor  $\alpha$  [TNF- $\alpha$ ] among them), consequent to the activation of an innate response. To achieve hepatocyte transduction with reduced acute toxicity, several strategies have been suggested, such as PEGylation of Ad vectors, which resulted in an extremely significant reduction in serum cytokines levels after vector administration, compared with naive Ad vectors.<sup>32,45,46</sup>

Pretreatment of animals can also reduce toxicity after IV administration of Ad vectors. TNF- $\alpha$  inhibitors have been shown to reduce the innate response and the consequent decrease in platelet levels<sup>41</sup>; in another study, administration of a PEGylated Ad vector in combination with methylprednisolone, an anti-inflammatory glucocorticoid, significantly prevents increase in IL-6 levels.<sup>32</sup> Pretreatment with dexamethasone prior to Ad vector administration significantly reduces innate immune response.<sup>47</sup>

An alternative strategy to reduce systemic vector toxicity consists in delivery to alternative tissues, such as muscle, using tissue-restricted promoters, thereby minimizing exposure to immune system cells. This strategy has been used for the administration of Glybera, an AAV vector developed for the treatment of lipoprotein lipase deficiency, the first gene therapy drug approved for clinical use in both the European Union and the United States in 2012.<sup>48</sup> We and others have previously observed that tissue-restricted expression may reduce immune response against transgenes.<sup>49,50</sup>

In a previous study, we demonstrated efficient expression of an LDLR/Tf fusion protein after IV delivery of an HD-Ad vector; this route of administration allows efficient hepatocyte transduction; antigen.<sup>49</sup> We expressed the LDLR/Tf fusion protein under the control of the transthyretin promoter to restrict transgene expression to hepatocytes; this strategy resulted in a long-term expression of the LDLR/Tf fusion protein and absence of an immune response toward the transgene, resulting in a stable correction of the lipid profile for the entire duration of the experiment and a significant reduction in aortic atherosclerosis in treated mice.<sup>28</sup>

To avoid the toxicity associated with IV administration of Ad vectors, we decided to evaluate the efficacy of IM administration of an HD-Ad vector containing a cassette designed for the muscle-restricted expression of the transgene. We generated cassettes for the expression of murine and human fusion proteins, both driven by the muscle-specific mCK promoter; subsequently, we inserted these expression cassettes in HD-Ad vector backbones to develop the HD-Ad-mLdlr/mTf and HD-Ad-hLDLR/hTF vectors (Figure 1A). We used the muscle-specific mCK promoter to try to reduce the development of antibodies against the fusion protein.

We generated codon-optimized cDNAs for both human and murine fusion proteins and evaluated their expression in differentiated C2C12, a murine myoblastoid cell line (Figure 1B). We observed the expression of both human and murine proteins; both were able

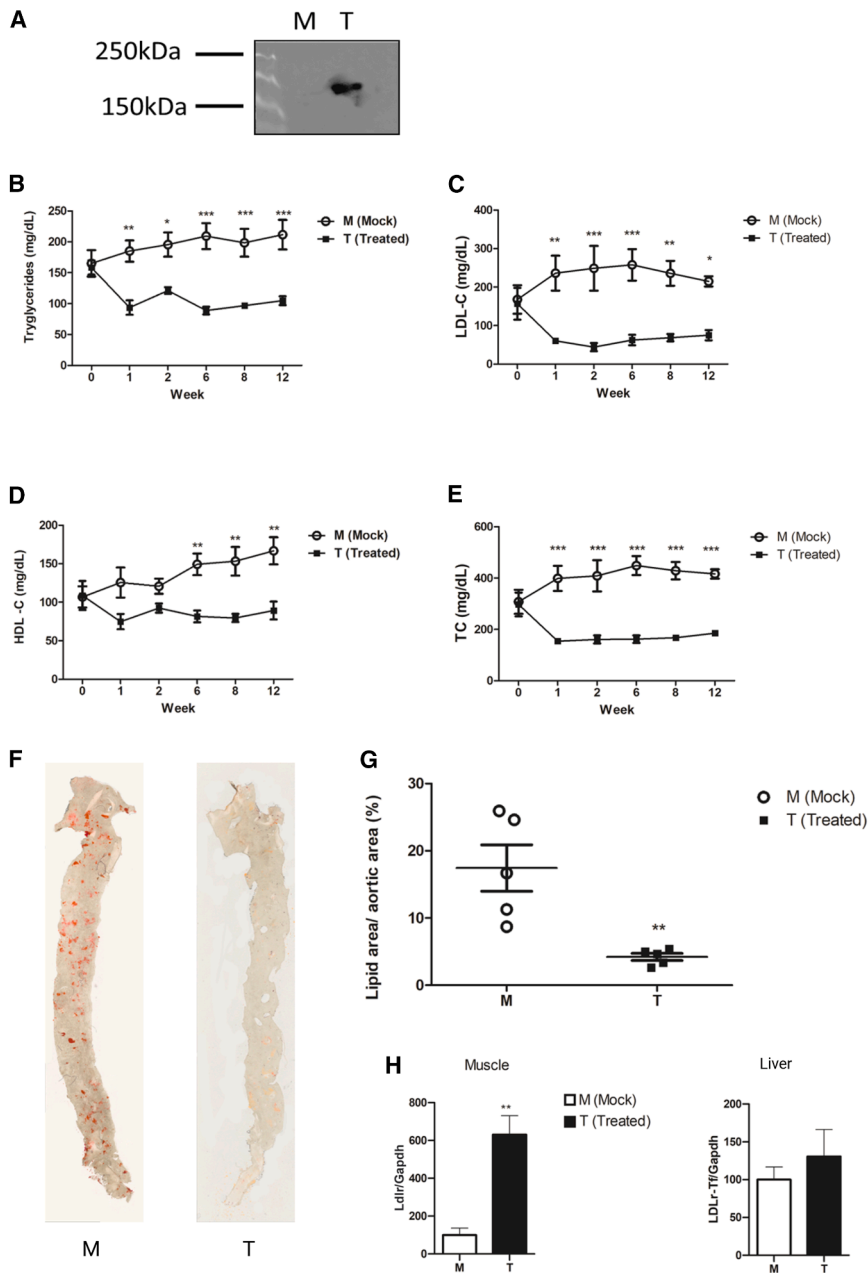


**Figure 3. Intramuscular administration of HD-Ad-mLdlr/mTf induces Ldlr/Tf serum secretion with a consequent improvement in the lipid profile and reduction of aortic atherosclerosis in Ldlr-deficient mice**

Two groups of Ldlr-deficient mice ( $n = 5$ ) were treated IM with either  $1.0 \times 10^{13}$  vp/kg of HD-Ad-mLdlr/mTf or with the same volume of PBS as control. The sample was collected before the treatments and 1, 2, 6, 8, and 12 weeks after treatments. (A) The Ldlr-Tf fusion protein was detected in blood samples 1 week after treatment in mice by western blot analysis using an anti-mouse Ldlr antibody. A band of approximately 170 kDa was observed in the plasma of mice treated with HD-Ad-mLdlr/mTf (T) but was absent in the plasma from untreated control mice (M). (B–E) (B) TG, (C) LDL, (D) HDL-C, and (E) TC levels were determined in both groups as mg/dL. Profiles were significantly different between treated and untreated mice ( $*p < 0.05$ ;  $**p < 0.01$ ;  $***p < 0.001$ ). (F) Twelve weeks after treatments, mice were sacrificed, and their aortas were dissected. Sub-intimal fat deposits in the aorta was determined after removal of external fat and staining with ORO. We observed fewer and smaller lipid deposits in aortas from treated mice compared with aortas from untreated animals. (G) Lesion areas in all the experimental mice were measured using ZEN 3.5 blue edition (Zeiss) and were reported as the percentage of lesion areas (lipid deposits area stained with ORO) in the total aortic surface. Data are reported as mean  $\pm$  SEM. (H) Tissue-specific expression of the fusion protein 1 week post-treatment, detected in skeletal muscle but not in liver by quantitative real-time PCR ( $**p = 0.0031$ ). Data are reported as mean  $\pm$  SEM.

to complement LDLR activity, restoring fluorescent 1,1'-dioctadecyl-3,3,3',3'-tetramethylindocarbocyanine perchlorate (DiI)-LDL uptake in CH01dIA7, an Ldlr-deficient cell line (Figures 1C and 1D). These data confirmed that we were able to achieve expression of both human and murine fusion protein after infection of differentiated myoblastoid cells; in addition, both transgenes were able to restore LDLR activity *in vitro*.

We then evaluated the efficacy of the IM administration of HD-Ad-mLdlr/mTf in inducing the expression of mLdlr/mTf in Ldlr-deficient mice and the efficacy of the fusion protein in

ameliorating lipid profile and reducing aortic atherosclerosis. We observed a significant amelioration in the lipid profile with a consequent reduction in aortic atherosclerosis in treated mice compared with untreated controls. We observed an overall decrease in HDL, LDL-C, TG, and TC levels in treated mice compared with the control group that lasted for the entire duration of the experiment (12 weeks, Figures 3A–3D). Aortic atherosclerosis lesion size confirmed the efficacy of the treatment: 12 weeks after administration, we observed a significant reduction in aortic atherosclerotic lesions in treated mice compared with controls (Figures 3E and 3F). These data indicate that a single IM administration of an HD-Ad vector expressing Ldlr/Tf has stable benefits in improving the lipid profile in Ldlr-deficient mice, with a consequent reduction in aortic atherosclerosis. While in human FH patients, tendon xanthomas and corneal arcus are associated with an increased risk of atherosclerotic cardiovascular disease, their observation in mice is not fully consistent, and often, specific conditions are required, making aortic atherosclerosis a

more sensitive and easily quantifiable endpoint for evaluating therapeutic efficacy.<sup>51</sup>

We observed stable amelioration of the lipid profile for 12 weeks, indicating a stable and effective transgene expression. Immune response against the transgene is usually developed in the first 1–2 weeks after administration and results in antibody response and absence of transgene efficacy within 1 month after administration.<sup>19,52</sup>

We evaluated host response after treatment, observing negligible systemic toxicity; indeed, plasma levels of IL-6 and IL-2 of treated mice were similar to those observed in untreated animals (Figures 2B and 2C). Similarly, D-dimer plasma levels were comparable in both groups, suggesting the absence of thrombotic disorders 6 h after viral administration (Figure 2D). Additionally, 72 h after IM vector administration, we did not observe any increase in AST or ALT levels, as observed in the control group, suggesting negligible liver toxicity (Figures 2E and 2F); hepatotoxicity was not observed during the entire duration of the experiment (Figures 2G and 2H; Table 1). Therefore, our data demonstrate that the muscle-restricted expression of the *Ldlr*/Tf fusion protein after IM administration of an HD-Ad vector results in phenotype correction *in vitro*, amelioration of lipid profile, and reduction in aortic atherosclerosis in *Ldlr*-deficient mice in the absence of a significant systemic host response and hepatic short- and long-term cytotoxicity (Figure 3).

These data indicate that IM administration of an HD-Ad vector expressing the *Ldlr*/Tf fusion protein may be more effective therapy for FH patients, rather than as a lifelong treatment. A relevant characteristic of this approach is the absence of the requirement for residual LDLR activity, different from all the strategies based on PCSK9 inhibition.<sup>27</sup> Therefore, patients unresponsive to PCSK9 inhibitors may benefit from this treatment. PCSK9 inhibition and LDLR/TF protein expression are strategies that act on different points of LDL metabolism; our strategy consists of the replacement of LDLR activity, whereas PCSK9 inhibition increases residual LDLR activity and may result in an increase in LDLR/TF activity. Therefore, our strategy is extremely relevant for patients unresponsive to PCSK9 inhibitors but is potentially additive, if not synergistic, for patients who respond to PCSK9 inhibitors without reaching a satisfactory lipid profile. Furthermore, IM delivery of HD-Ad expressing LDLR/TF could be extended to other models of FH, including PCSK9-null animals or models with different genetic etiologies. Muscle-directed gene therapy offers the advantage of systemic secretion of the therapeutic protein independent of endogenous liver function, which may be particularly valuable across different FH genotypes where hepatic LDL receptor pathways are absent or dysfunctional. Compared with liver-directed gene therapy, muscle-directed delivery triggers only a transient, localized immune response, limits systemic vector exposure, and reduces hepatotoxicity, while it allows persistent systemic secretion of the therapeutic protein.<sup>44,53</sup> These features suggest that muscle-directed HD-Ad may represent a more broadly appli-

cable strategy for the treatment of diverse FH genotypes, complementing established liver-targeted approaches. Although these characteristics support the potential safety of muscle-directed HD-Ad administration, the present study did not include a detailed evaluation of muscle tissue integrity or local inflammatory responses following IM injection. Future studies will be required to address these aspects and to further define the long-term safety profile of this delivery route.

## MATERIALS AND METHODS

### Development of HD-Ad vectors for expression of murine and human fusion protein

We engineered muscle-specific expression cassettes for human and murine fusion protein. *Cl*I and *S*a*C*I (New England Biolabs) sites were added, and the sequence was initially inserted into pUC57 and then subcloned into the pLPBL1 shuttle vector (with flanking *Asc*I sites). The mCK promoter was excised from pBS-mCK (Addgene) via *X*hoI (New England Biolabs) digestion and inserted to generate the final pLPBL1-mCK-m*Ldlr*/mTf cassette, which was confirmed by Sanger sequencing. Similarly, a human chimeric construct (incorporating hLDLR, hTF, WPRE, and an SV40 polyadenylation signal) was designed *in silico* and cloned into the pcDNA3.1<sup>+</sup> vector with the mCK promoter obtained from ProteoGenix. Both expression cassettes were excised with *Asc*I (New England Biolabs), ligated into the pΔ21 (HD-Ad) backbone, transformed into electrocompetent *Escherichia coli*, and the resulting clones verified by sequencing.

### Tissue cultures and transfections

The 116 cells (provided by Dr. Ng, Baylor College of Medicine, Houston, TX) were cultured in  $\alpha$ -minimal essential medium (MEM, Gibco) containing 10% fetal bovine serum (FBS, Gibco), 1% 50 U penicillin and 50  $\mu$ g streptomycin (P/S, MicroGEM), and 4 mM L-glutamine (L-Gln, Gibco) in a humidified incubator at 37°C with 5% of CO<sub>2</sub>. For suspension cultures, 116 cells were cultured in S-MEM (Gibco) containing 10% FBS, 1% 50 U penicillin and 50  $\mu$ g streptomycin (P/S, MicroGEM), and 4 mM L-Gln (Gibco) in a humidified incubator at 37°C with 5% CO<sub>2</sub>.

C2C12 cells were cultured in DMEM (Gibco) supplemented with 10% FBS, 2% L-Gln, and 1% P/S. C2C12 myogenic differentiation was carried out by plating cells at a  $2 \times 10^4$  cell/cm<sup>2</sup> density in DMEM, switching to differentiation medium (DMEM-high glucose without sodium pyruvate, Gibco), 2% horse serum (Gibco), 1% L-Gln, and 1% P/S after 24 h, replacing it every 1–2 days. A switch from a myoblast round shape to an elongated tubular shape was observed 72 h after treatment.

The CHOld1A7 cell line was cultured in  $\alpha$ -MEM medium (Sigma-Aldrich) supplemented with 10% FBS and 1% L-Gln.

We transfected 116 cells with Lipofectamine 2000 (Life Technologies); C2C12 cells were transfected with Viafect transfection reagent (Promega) in both cases following the manufacturer's instructions.

### HD-Ad vectors production and purification

Rescue and amplification of the HD-Ad vectors were performed using Ad-NG163R-2 helper virus (HV).<sup>33,54,55</sup> HD-Ad-mLdlr/mTf and HD-Ad-hLDLR/hTF vectors were produced by transfecting with Lipofectamine 2000 (Invitrogen) 10  $\mu$ g of PmeI-digested of either pHD-Ad-mLdlr/mTf or pHD-Ad-hLDLR/hTF plasmids in 116 cells at 70%–80% of confluence in a 60-mm dishes. The following day, transfected cells were over-infected with HV (50 PFU/cell).

Vectors were amplified by serial co-infection of 116 cells at 80% confluence in 60-mm dishes with 10% of crude lysate from the previous passage and HV at 10 PFU/cell; after 3 passages (P3) in 60-mm dishes, 116 cells at 80% confluence were co-infected with 10% of crude serial P3 lysate and 10 PFU/cell of HV in a 150-mm dish for P4. Both HD-Ad vectors were then produced in large scale in a 3-L suspension culture of 116 cells ( $3\text{--}4 \times 10^5$  cells/mL) in spinner flasks co-infected with the crude lysate obtained in P4 with HV (25 PFU/cell). Cells from suspension cultures were collected 2 days after infection and subsequently lysed with three freeze-thaw cycles.

For vector purification, cellular debris was spun down, and lysates were subject to ultracentrifugation in a CsCl gradient (2.5 mL 1.45 g/mL and 3 mL 1.25 g/mL CsCl solutions) for 1 h at 27,000 rpm at 4°C, with minimum acceleration and deceleration. The vectors were collected, and ultracentrifugation was repeated in the same conditions for 20 h. Vectors were then dialyzed in 800 mL TM solution (10 mM Tris-HCl pH 8.0, 2 mM MgCl<sub>2</sub>) for 2 h. TM solution was then substituted with freezing solution (10 mM Tris-HCl pH 8.0, 2 mM MgCl<sub>2</sub>, 4% sucrose) and dialyzed overnight. The following day, vectors were collected, aliquoted, and stored at  $-80^\circ\text{C}$ .<sup>56</sup> Vector concentration was determined as vp/mL, measuring absorbance at 260 nm, as described elsewhere.<sup>57</sup>

### Western blot analysis

C2C12 were differentiated as previously described and infected with 100 MOIs with HD-Ad-mLdlr/mTf or HD-Ad-hLDLR/hTF; cells were collected 48 h after infection and centrifuged at 1,000 rpm for 5 min at room temperature. Cell pellets were then suspended in lysis buffer (1 mM EDTA, 50 mM Tris-HCl pH 7.5, 70 mM NaCl, 1% Triton X-100), 5 mM sodium fluoride (NaF), and  $1 \times$  protease inhibitors (Roche) and incubated on ice for 30 min. Samples were then centrifuged at 1,300 rpm for 15 min at 4°C, and the suspension containing total cell protein was collected. Proteins were quantified using Bradford assay (Bio-Rad) and loaded on a 10% SDS-polyacrylamide gel. Then, they were electrophoretically transferred onto an ImmunoBlot polyvinylidene fluoride membrane (Bio-Rad). Membranes were incubated for 1 h at room temperature in blocking buffer (Tris-buffered saline containing 6% blocking grade blocker, non-fat dry milk; Bio-Rad) to block non-specific protein binding sites and incubated at 4°C overnight with the primary antibody anti-rabbit- $\alpha$ -mLDLR (Abcam) diluted 1:500 in blocking buffer. Secondary antibody binding was visualized with an enhanced chemiluminescence (ECL) western blotting detection system (Pierce ECL Plus, Thermo and Clarity ECL substrate, Bio-Rad) according to

the manufacturers' instructions. Blood samples were collected and centrifuged to obtain serum. From each mouse, 30  $\mu$ L serum were pooled and concentrated using Amicon Ultra centrifugal filters with a 100-kDa molecular weight cutoff (catalog no. UFC510024, Merck KGaA). Once a final volume of approximately 20  $\mu$ L was reached, samples were mixed with Laemmli sample buffer, boiled, and loaded onto 10% precast gels for electrophoresis (catalog no. 4568033, Bio-Rad). For detection, membranes (catalog no. 1704156EDU, Bio-Rad) were incubated with an anti-LDLR primary antibody (catalog no. ab52818, Abcam), followed by goat anti-rabbit immunoglobulin G horseradish peroxidase (HRP) conjugated secondary antibody (catalog no. 7074, Cell Signaling Technology). Signal visualization was performed using Clarity Max ECL substrate (catalog no. 1705062, Bio-Rad).

### Fluorescent LDL incorporation assay

CHOIdIA7 cells were plated at  $5 \times 10^4$  cells per well density on glass coverslips in a 24-well plate. The day after, cells were cultured in a lipoprotein-deprived serum media. After 24 h, cells were treated with the supernatant obtained from C2C12 infected with HD-Ad-mLdlr/mTf, HD-Ad-hLDLR/hTF, or an empty HD-Ad vector for 1 h, and fluorescent-labeled LDLs (DiI-LDL, Molecular Probe by Life Technologies) were added to the media at a 5- $\mu$ g/mL concentration for a 5-h incubation. Cells were then washed 3 times with PBS at room temperature and fixed using a 4% paraformaldehyde/PBS solution for 15 min at room temperature. After 5 washes with PBS, cells were incubated with DAPI (Thermo Scientific) for 5 min. Incorporation of DiI-LDLs in cells was evaluated by confocal microscopy with 20 $\times$  and 60 $\times$  objectives (LSM 980 confocal, Zeiss).

### Animal studies

Animal studies were performed following National Institutes of Health guidelines, ethics, and safety rules, and guidelines for the use in biomedical research provided by relevant Italian law and European Union directives (no. 86/609/EC). The Italian Minister of Health approved these studies (no. 588/2022-PR). All efforts were made to minimize animals' suffering. Food and water were provided *ad libitum*. The experiments were performed in 8-week-old *Ldlr*-deficient mice in C57BL/6 background provided by Charles River Laboratory. Mice were treated with a single IM administration of  $1 \times 10^{13}$  vp/kg of the HD-Ad-mLdlr/mTf vector diluted in PBS in a total volume of 100  $\mu$ L; control mice were treated with an equal volume of PBS. Viral injections were performed in a total volume of 100  $\mu$ L. To optimize delivery, this volume was divided into two separate injections of 50  $\mu$ L each, administered into the same leg muscle of the mice. Blood samples were collected in a 0.5-mL EDTA tube (Greiner Bio-One) at 0, 1, 2, 4, 8, and 12 weeks from retro-orbital plexus and centrifuged at 2,000 rpm for 15 min to obtain plasma. We determined plasma lipid profile TG, TC and HDL-C using a Vitros 250 Analyzer (Ortho Clinical Diagnostic, Johnson & Johnson). LDL-C was calculated as (TC levels – HDL-C levels) – (TG/5). To evaluate short toxicity and hepatic toxicity, blood samples were collected in 1.5-mL EDTA-coated tubes at 6 h and 3, 14, 56, and

84 days after treatment. AST and ALT plasma levels were determined using the Vitros 250 Analyzer.

### ELISAs

Determinations of plasma IL-6 (catalog no. MODL00714, AssayGenie), IL-12 (catalog no. SBRS1412, AssayGenie), and D-dimer (catalog no. MODL00348, AssayGenie) were made via enzyme-linked immunosorbent assay (ELISA) according to the manufacturer's instructions. In summary, the plate was washed twice with 1 × wash buffer (WB) and then loaded with 100 μL of the appropriate standard at different dilutions to obtain a standard curve. We loaded 100 μL of each plasma sample onto the plate in duplicate. Then, the plate was incubated for 90 min at 37°C in the dark and washed three times with WB. We added 100 μL of a solution containing the appropriate target antibody to each well, incubated them for 60 min at 37°C in the dark, and washed three times with WB. Subsequently, 100 μL of a solution containing HRP-streptavidin conjugate was added to each well and incubated for 30 min at 37°C in the dark. At the end of the incubation, the plate was washed 5 times with WB, and 90 μL of a solution containing 3,3',5,5'-tetramethylbenzidine substrate was added to each well and incubated in the dark at least for 20 min at 37°C. When the well color turned to blue, 50 μL of stop solution was added to each well, and the absorbance at 450 nm was immediately read using a plate reader (PerkinElmer, catalog no. 2102).

### Quantitative real-time PCR

Total RNA was extracted from skeletal muscle and liver tissues collected from five untreated mice and five mice injected IM with  $1 \times 10^{13}$  vp/kg HD-Ad-mLdlr/mTf using TRIzol reagent (Thermo Fisher Scientific), according to the manufacturer's instructions. RNA concentration and purity were determined spectrophotometrically. For cDNA synthesis, 2 μg of total RNA per sample was reverse transcribed using the SensiFAST cDNA Synthesis Kit (Meridian Bioscience) following the manufacturer's protocol. Quantitative real-time PCR was performed using 80 ng cDNA per reaction well with the SensiFAST SYBR Hi-ROX Kit (Meridian Bioscience). Amplification was carried out on a QuantStudio 6 Pro Real-Time PCR System (Applied Biosystems). The following primers were used: *Ldlr*-Tf forward primer, 5'-TGGCCAGCGTGACCGT-3'; *Ldlr*-Tf reverse primer, 5'-GAAGCTGATGCACTTGGTGT-3'; glyceraldehyde 3-phosphate dehydrogenase (*Gapdh*) forward primer, 5'-CATCACTGCCACCCAGAAGACTG-3'; and *Gapdh* reverse primer, 5'-ATGCCAGTGAGCTTCCCCTTCAG-3'. *Gapdh* was used as the internal reference gene for the normalization of gene expression. Relative mRNA expression levels were calculated using the comparative Ct ( $\Delta\Delta C_t$ ) method.

### Aortic atherosclerosis lesion quantification

After sacrifice of the experimental mice, aortas were dissected from the heart to iliac branching, removing the external fat to stain exclusively sub-intima aortic fat.<sup>58</sup> Aortic lesion staining was performed as previously described.<sup>31,58</sup> The aorta images were acquired with confocal microscopy using a 10× objective on the MICA (micro-

hub platform, Leica), and atherosclerotic lesions were measured through ZEN 3.5 blue edition. The percentage of the atherosclerotic area was evaluated with the formula (lesion area/aorta area) × 100% = ORO surface area (percentage of total).<sup>58</sup>

### Statistical analyses

Statistical analyses were performed using GraphPad Prism 5.02 for Windows (GraphPad Software), as detailed in each figure legend. One-way ANOVA was used to assess differences in D-dimer, IL-6, and IL-12 levels between untreated and IM-treated mice. To compare lipid profiles between treated and untreated plasma samples, statistical significance was determined using two-way ANOVA. Differences in the percentage of aortic atherosclerotic areas were analyzed using a two-tailed Student's *t* test, as indicated in the figure legends. A *p* value <0.05 was considered statistically significant.

### DATA AND CODE AVAILABILITY

The datasets generated during this study are available from the corresponding author upon reasonable request.

### ACKNOWLEDGMENTS

The author wishes to acknowledge Dr. Ciro Barile and Domenico Sorrentino for their expert assistance in animal studies. This work was realized using the CEINGE-Biotecnologie Avanzate Franco Salvatore Institute shared facilities, advanced light microscopy, and laboratory. The study was supported by the Spoke 8 of the Italian National Center for Gene Therapy and Drugs based on RNA Technology (project code CN00000041), by funding program of Progetti di Ricerca di Rilevante Interesse Nazionale (PRIN) "Assessment of clinical, genetic and biochemical determinants of cardiovascular risk to improve" (project code 20225JX495) and by funding program of Italian National Recovery and Resilience Plan "Development of innovative therapeutic strategies for the treatment of Familial Hypercholesterolemia" (PRIN-PNRR project code P20224C95A) funded by the Italian Ministry of University and Research (MUR). The figures were created using BioRender. Support was obtained by Extend, a National Technology Transfer Biotech Hub launched by C&D Venture Capital.

### AUTHOR CONTRIBUTIONS

Study concept and design, M.V., F.S., L.T., and L.P.; data collection and analysis, A.D., M.V., F.S., and L.C.; data interpretation, M.V., F.S., L.C., and L.P.; manuscript preparation, M.V., F.S., and L.P.; critical revision, A.B., R.P., G.C., V.C., and L.P. All authors listed have made a substantial, direct, and intellectual contribution to the work and approved it for publication.

### DECLARATION OF INTERESTS

M.V., L.P., and L.T. are founders of Kimera s.r.l.

### REFERENCES

1. Mainieri, F., Tagi, V.M., and Chiarelli, F. (2022). Recent Advances on Familial Hypercholesterolemia in Children and Adolescents. *Biomedicines* 10, 1043.
2. Berberich, A.J., and Hegele, R.A. (2019). The complex molecular genetics of familial hypercholesterolaemia. *Nat. Rev. Cardiol.* 16, 9–20.
3. Representatives of the Global Familial Hypercholesterolemia Community, Wilemon, K.A., Patel, J., Aguilar-Salinas, C., Ahmed, C.D., Alkhnifawi, M., Almahmeed, W., Alonso, R., Al-Rasadi, K., Badimon, L., et al. (2020). Reducing the Clinical and Public Health Burden of Familial Hypercholesterolemia: A Global Call to Action. *JAMA Cardiol.* 5, 217–229.
4. Borén, J., Chapman, M.J., Krauss, R.M., Packard, C.J., Bentzon, J.F., Binder, C.J., Daemen, M.J., Demer, L.L., Hegele, R.A., Nicholls, S.J., et al. (2020). Low-density lipoproteins cause atherosclerotic cardiovascular disease: Pathophysiological, genetic,

- and therapeutic insights: A consensus statement from the European Atherosclerosis Society Consensus Panel. *Eur. Heart J.* *41*, 2313–2330.
5. Sniderman, A.D., Tsimikas, S., and Fazio, S. (2014). The severe hypercholesterolemia phenotype: Clinical diagnosis, management, and emerging therapies. *J. Am. Coll. Cardiol.* *63*, 1935–1947.
  6. May, P., Herz, J., and Bock, H.H. (2005). Molecular mechanisms of lipoprotein receptor signalling. *Cell. Mol. Life Sci.* *62*, 2325–2338.
  7. Siddiqui, H., Yevstigneyev, N., Madani, G., and McCormick, S. (2022). Approaches to Visualising Endocytosis of LDL-Related Lipoproteins. *Biomolecules* *12*, 158.
  8. Razzini, G., Parise, F., Calebri, D., Battini, R., Bagni, B., Corazzari, T., Tarugi, P., Angelelli, C., Molinari, S., Falqui, L., and Ferrari, S. (2004). Fusion Protein : In Vivo Production and Functional Evaluation as a Potential Therapeutic Tool for Lowering Plasma LDL Cholesterol. *Hum. Gene Ther.* *15*, 533–541.
  9. Hymel, D., and Peterson, B.R. (2012). Synthetic cell surface receptors for delivery of therapeutics and probes. *Adv. Drug Deliv. Rev.* *64*, 797–810.
  10. Defesche, J.C., Gidding, S.S., Harada-Shiba, M., Hegele, R.A., Santos, R.D., and Wierzbicki, A.S. (2017). Familial hypercholesterolaemia. *Nat. Rev. Dis. Primers* *3*, 17093.
  11. Arca, M., Celant, S., Olimpieri, P.P., Colatrella, A., Tomassini, L., D’Erasmus, L., Averna, M., Zambon, A., Catapano, A.L., Russo, P., et al. (2023). Real-World Effectiveness of PCSK9 Inhibitors in Reducing LDL-C in Patients With Familial Hypercholesterolemia in Italy: A Retrospective Cohort Study Based on the AIFA Monitoring Registries. *J. Am. Heart Assoc.* *12*, e026550.
  12. Rikhi, R., and Shapiro, M.D. (2022). Newer and Emerging LDL-C Lowering Agents and Implications for ASCVD Residual Risk. *J. Clin. Med.* *11*, 4611.
  13. Cuchel, M., Raal, F.J., Hegele, R.A., Al-Rasadi, K., Arca, M., Averna, M., Bruckert, E., Freiburger, T., Gaudet, D., Harada-Shiba, M., et al. (2023). 2023 Update on European Atherosclerosis Society Consensus Statement on Homozygous Familial Hypercholesterolaemia: New treatments and clinical guidance. *Eur. Heart J.* *44*, 2277–2291.
  14. Biolo, G., Vinci, P., Mangogna, A., Landolfo, M., Schincariol, P., Fiotti, N., Mearelli, F., and Di Girolamo, F.G. (2022). Mechanism of action and therapeutic use of bempedoic acid in atherosclerosis and metabolic syndrome. *Front. Cardiovasc. Med.* *9*, 1028355.
  15. Björkegren, J.L.M., and Lusis, A.J. (2022). Atherosclerosis: Recent developments. *Cell* *185*, 1630–1645. <https://doi.org/10.1016/j.cell.2022.04.004>.
  16. Zou, L., Zhou, H., Pastore, L., and Yang, K. (2000). Prolonged transgene expression mediated by a helper-dependent adenoviral vector (hdAd) in the central nervous system. *Mol. Ther.* *2*, 105–113.
  17. Pastore, L., Belalcazar, L.M., Oka, K., Cela, R., Lee, B., Chan, L., and Beaudet, A.L. (2004). Helper-dependent adenoviral vector-mediated long-term expression of human apolipoprotein A-I reduces atherosclerosis in apo E-deficient mice. *Gene* *327*, 153–160.
  18. Belalcazar, L.M., Merched, A., Carr, B., Oka, K., Chen, K.H., Pastore, L., Beaudet, A., and Chan, L. (2003). Long-term stable expression of human apolipoprotein A-I mediated by helper-dependent adenovirus gene transfer inhibits atherosclerosis progression and remodels atherosclerotic plaques in a mouse model of familial hypercholesterolemia. *Circulation* *107*, 2726–2732.
  19. Oka, K., Pastore, L., Kim, I.H., Merched, A., Nomura, S., Lee, H.J., Merched-Sauvage, M., Arden-Riley, C., Lee, B., Finegold, M., et al. (2001). Long-term stable correction of low-density lipoprotein receptor-deficient mice with a helper-dependent adenoviral vector expressing the very low-density lipoprotein receptor. *Circulation* *103*, 1274–1281.
  20. Conroy, G. (2022). How gene therapy is emerging from its ‘dark age’. *Nature* *612*, S24–S26.
  21. Bueren, J.A., and Auricchio, A. (2023). Advances and Challenges in the Development of Gene Therapy Medicinal Products for Rare Diseases. *Hum. Gene Ther.* *34*, 763–775.
  22. Tripodi, L., Sasso, E., Feola, S., Coluccino, L., Vitale, M., Leoni, G., Szomolay, B., Pastore, L., and Cerullo, V. (2023). Systems Biology Approaches for the Improvement of Oncolytic Virus-Based Immunotherapies. *Cancers* *15*, 1297.
  23. Wang, C., Pan, C., Yong, H., Wang, F., Bo, T., Zhao, Y., Ma, B., He, W., and Li, M. (2023). Emerging non-viral vectors for gene delivery. *J. Nanobiotechnology* *21*, 272.
  24. Wilson, J.M., and Grossman, M. (1993). Therapeutic strategies for familial hypercholesterolemia based on somatic gene transfer. *Am. J. Cardiol.* *72*, 59D–63D.
  25. Aravalli, R.N., Belcher, J.D., and Steer, C.J. (2015). Liver-targeted gene therapy: Approaches and challenges. *Liver Transpl.* *21*, 718–737.
  26. Al-Allaf, F.A., Coutelle, C., Waddington, S.N., David, A.L., Harbottle, R., and Themis, M. (2010). LDLR-Gene therapy for familial hypercholesterolaemia: Problems, progress, and perspectives. *Int. Arch. Med.* *3*, 36.
  27. Leggiero, E., Astone, D., Cerullo, V., Lombardo, B., Mazzaccara, C., Labruna, G., Sacchetti, L., Salvatore, F., Croyle, M., Pastore, L., et al. (2013). PEGylated helper-dependent adenoviral vector expressing human Apo A-I for gene therapy in LDLR-deficient mice This article has been corrected since online publication and a corrigendum is also printed in this issue. *Gene Ther.* *20*, 1124–1130.
  28. Leggiero, E., Labruna, G., Iaffaldano, L., Lombardo, B., Greco, A., Fiorenza, D., Gramanzini, M., Montanaro, D., Baldi, A., Cerullo, V., et al. (2019). Helper-dependent adenovirus-mediated gene transfer of a secreted LDL receptor/transferrin chimeric protein reduces aortic atherosclerosis in LDL receptor-deficient mice. *Gene Ther.* *26*, 121–130.
  29. Gordon, S.M., Li, H., Zhu, X., Shah, A.S., Lu, L.J., and Davidson, W.S. (2015). A comparison of the mouse and human lipoproteome: suitability of the mouse model for studies of human lipoproteins. *J. Proteome Res.* *14*, 2686–2695.
  30. Wilson, J.M., Chowdhury, N.R., Grossman, M., Wajsman, R., Epstein, A., Mulligan, R.C., and Chowdhury, J.R. (1990). Temporary amelioration of hyperlipidemia in low density lipoprotein receptor-deficient rabbits transplanted with genetically modified hepatocytes. *Proc. Natl. Acad. Sci. USA* *87*, 8437–8441.
  31. Oka, K., Mullins, C.E., Kushwaha, R.S., Leen, A.M., and Chan, L. (2015). Gene therapy for rhesus monkeys heterozygous for LDL receptor deficiency by balloon catheter hepatic delivery of helper-dependent adenoviral vector. *Gene Ther.* *22*, 87–95.
  32. Croyle, M.A., Le, H.T., Linse, K.D., Cerullo, V., Toietta, G., Beaudet, A., and Pastore, L. (2005). PEGylated helper-dependent adenoviral vectors: Highly efficient vectors with an enhanced safety profile. *Gene Ther.* *12*, 579–587.
  33. Rosewell, A., Vetrini, F., and Ng, P. (2011). Helper-Dependent Adenoviral Vectors. *J. Genet. Syndr. Gene Ther.* *5*, 001.
  34. Kim, I.H., Józkwicz, A., Piedra, P.A., Oka, K., and Chan, L. (2001). Lifetime correction of genetic deficiency in mice with a single injection of helper-dependent adenoviral vector. *Proc. Natl. Acad. Sci. USA* *98*, 13282–13287.
  35. Toietta, G., Mane, V.P., Norona, W.S., Finegold, M.J., Ng, P., McDonagh, A.F., Beaudet, A.L., and Lee, B. (2005). Lifelong elimination of hyperbilirubinemia in the Gunn rat with a single injection of helper-dependent adenoviral vector. *Proc. Natl. Acad. Sci. USA* *102*, 3930–3935.
  36. Greig, J.A., Limberis, M.P., Bell, P., Chen, S.J., Calcedo, R., Rader, D.J., and Wilson, J.M. (2017). Non-Clinical Study Examining AAV8.TBG.hLDLR Vector-Associated Toxicity in Chow-Fed Wild-Type and LDLR+/- Rhesus Macaques. *Hum. Gene Ther. Clin. Dev.* *28*, 39–50.
  37. Greig, J.A., Limberis, M.P., Bell, P., Chen, S.J., Calcedo, R., Rader, D.J., and Wilson, J.M. (2017). Nonclinical Pharmacology/Toxicology Study of AAV8.TBG.mLDLR and AAV8.TBG.hLDLR in a Mouse Model of Homozygous Familial Hypercholesterolemia. *Hum. Gene Ther. Clin. Dev.* *28*, 28–38.
  38. Vandamme, C., Adjali, O., and Mingozzi, F. (2017). Unraveling the Complex Story of Immune Responses to AAV Vectors Trial After Trial. *Hum. Gene Ther.* *28*, 1061–1074.
  39. Hordeaux, J., Wang, Q., Katz, N., Buza, E.L., Bell, P., and Wilson, J.M. (2018). The Neurotropic Properties of AAV-PHP.B Are Limited to C57BL/6J Mice. *Mol. Ther.* *26*, 664–668.
  40. O’Neal, W.K., Zhou, H., Morral, N., Langston, C., Parks, R.J., Graham, F.L., Kochanek, S., and Beaudet, A.L. (2000). Toxicity associated with repeated administration of first-generation adenovirus vectors does not occur with a helper-dependent vector. *Mol. Med.* *6*, 179–195.
  41. Mane, V.P., Toietta, G., McCormack, W.M., Conde, I., Clarke, C., Palmer, D., Finegold, M.J., Pastore, L., Ng, P., Lopez, J., and Lee, B. (2006). Modulation of

- TNF  $\alpha$ , a determinant of acute toxicity associated with systemic delivery of first-generation and helper-dependent adenoviral vectors. *Gene Ther.* *13*, 1272–1280.
42. Capasso, C., Garofalo, M., Hirvonen, M., and Cerullo, V. (2014). The evolution of adenoviral vectors through genetic and chemical surface modifications. *Viruses* *6*, 832–855.
  43. Brunetti-Pierri, N., Palmer, D.J., Beaudet, A.L., Carey, K.D., Finegold, M., and Ng, P. (2004). Acute Toxicity After High-Dose Systemic Injection of Helper-Dependent Adenoviral Vectors into Nonhuman Primates. *Hum. Gene Ther.* *15*, 35–46.
  44. Muruve, D.A., Cotter, M.J., Zaiss, A.K., White, L.R., Liu, Q., Chan, T., Clark, S.A., Ross, P.J., Meulenbroek, R.A., Maelandsmo, G.M., and Parks, R.J. (2004). Helper-Dependent Adenovirus Vectors Elicit Intact Innate but Attenuated Adaptive Host Immune Responses In Vivo. *J. Virol.* *78*, 5966–5972.
  45. Wonganan, P., Clemens, C.C., Brasky, K., Pastore, L., and Croyle, M.A. (2011). Species differences in the pharmacology and toxicology of PEGylated helper-dependent adenovirus. *Mol. Pharm.* *8*, 78–92.
  46. Hofherr, S.E., Mok, H., Gushiken, F.C., Lopez, J.A., and Barry, M.A. (2007). Polyethylene glycol modification of adenovirus reduces platelet activation, endothelial cell activation, and thrombocytopenia. *Hum. Gene Ther.* *18*, 837–848.
  47. Seregin, S.S., Appledorn, D.M., McBride, A.J., Schuldt, N.J., Aldhamen, Y.A., Voss, T., Wei, J., Bujold, M., Nance, W., Godbehere, S., and Amalfitano, A. (2009). Transient Pretreatment With Glucocorticoid Ablates Innate Toxicity of Systemically Delivered Adenoviral Vectors Without Reducing Efficacy. *Mol. Ther.* *17*, 685–696.
  48. Ferreira, V., Petry, H., and Salmon, F. (2014). Immune Responses to AAV-Vectors, the Glybera Example from Bench to Bedside. *Front. Immunol.* *5*, 82.
  49. Pastore, L., Morral, N., Zhou, H., Garcia, R., Parks, R.J., Kochanek, S., Graham, F.L., Lee, B., and Beaudet, A.L. (1999). Use of a liver-specific promoter reduces immune response to the transgene in adenoviral vectors. *Hum. Gene Ther.* *10*, 1773–1781.
  50. Wang, L., Takabe, K., Bidlingmaier, S.M., Ill, C.R., and Verma, I.M. (1999). Sustained correction of bleeding disorder in hemophilia B mice by gene therapy. *Proc. Natl. Acad. Sci. USA* *96*, 3906–3910.
  51. Liu, M.M., Peng, J., Guo, Y.L., Zhu, C.G., Wu, N.Q., Xu, R.X., Dong, Q., and Li, J.J. (2021). Relations of physical signs to genotype, lipid and inflammatory markers, coronary stenosis or calcification, and outcomes in patients with heterozygous familial hypercholesterolemia. *J. Transl. Med.* *19*, 498.
  52. Mingozzi, F., and High, K.A. (2013). Immune responses to AAV vectors: overcoming barriers to successful gene therapy. *Blood* *122*, 23–36.
  53. Maione, D., Della Rocca, C., Giannetti, P., D'Arrigo, R., Liberatoscioli, L., Franlin, L.L., Sandig, V., Ciliberto, G., La Monica, N., Savino, R., et al. (2001). An improved helper-dependent adenoviral vector allows persistent gene expression after intramuscular delivery and overcomes preexisting immunity to adenovirus. *Proc. Natl. Acad. Sci. USA* *98*, 5986–5991.
  54. Dormond, E., Meneses-Acosta, A., Jacob, D., Durocher, Y., Gilbert, R., Perrier, M., and Kamen, A. (2009). An efficient and scalable process for helper-dependent adenoviral vector production using polyethylenimine-adenofection. *Biotechnol. Bioeng.* *102*, 800–810.
  55. Zhou, H., Zhao, T., Pastore, L., Nageh, M., Zheng, W., Rao, X.M., and Beaudet, A.L. (2001). A Cre-Expressing Cell Line and an E1/E2a Double-Deleted Virus for Preparation of Helper-Dependent Adenovirus Vector. *Mol. Ther.* *3*, 613–622.
  56. Tripodi, L., Passariello, M., D'Argenio, V., Leggiero, E., Vitale, M., Colicchio, R., Salvatore, P., Cerullo, V., De Lorenzo, C., and Pastore, L. (2021). Evaluation of the antiproliferative effect of *Bifidobacterium longum* BB-536 in solid tumor cell lines, co-cultured with murine splenocytes. *Biochim. Clinica* *45*, 242–247.
  57. Sweeney, J.A., and Hennessey, J.P., Jr. (2002). Evaluation of accuracy and precision of adenovirus absorptivity at 260 nm under conditions of complete DNA disruption. *Virology* *295*, 284–288.
  58. Chen, P.Y., Qin, L., and Simons, M. (2022). Imaging and Analysis of Oil Red O-Stained Whole Aorta Lesions in an Aneurysm Hyperlipidemia Mouse Model. *J. Vis. Exp.* *183*, 61277. <https://doi.org/10.3791/61277>.